Disruption of Cytochrome c Oxidase Function Induces Warburg Effect and Metabolic Reprogramming

Satish Srinivasan[1], **Manti Guha**[1], **Dawei W Dong**[1], **Kelly A Whelan**[2], **Gordon Ruthel**[1], **Yasuto Uchikado**[3], **Shoji Natsugoe**[3], **Hiroshi Nakagawa**[2], and **Narayan G. Avadhani**[1,§]

[1]The Department of Biomedical Sciences, The Mari Lowe Center for Comparative Oncology, School of Veterinary Medicine, University of Pennsylvania, Philadelphia, PA 19104

[2]Division of Gastroenterology, Department of Medicine, Perelman School of Medicine, University of Pennsylvania, Philadelphia, PA 19104

[3]Department of Digestive Surgery, Breast and Thyroid Surgery, Graduate School of Medicine, Kagoshima University, Kagoshima 890-8520, Japan

Abstract

Defects in mitochondrial oxidative phosphorylation complexes, altered bioenergetics and metabolic shift are often seen in cancers. Here we show a role for the dysfunction of electron transport chain component, cytochrome c oxidase (CcO) in cancer progression. We show that genetic silencing of the CcO complex by shRNA expression and loss of CcO activity in multiple cell types from the mouse and human sources resulted in metabolic shift to glycolysis, loss of anchorage dependent growth and acquired invasive phenotypes. Disruption of CcO complex caused loss of transmembrane potential and induction of Ca^{2+}/Calcineurin-mediated retrograde signaling. Propagation of this signaling, includes activation of PI3-kinase, IGF1R and Akt, Ca^{2+} sensitive transcription factors and also, TGFβ1, MMP16, periostin that are involved in oncogenic progression. Whole genome expression analysis showed up regulation of genes involved in cell signaling, extracellular matrix interactions, cell morphogenesis, cell motility and migration. The transcription profiles reveal extensive similarity to retrograde signaling initiated by partial mtDNA depletion, though distinct differences are observed in signaling induced by CcO dysfunction. The possible CcO dysfunction as a biomarker for cancer progression was supported by data showing that esophageal tumors from human patients show reduced CcO subunits IVi1 and Vb in regions that were previously shown to be hypoxic core of the tumors. Our results show that mitochondrial electron transport chain defect initiates a retrograde signaling. These results suggest that a defect in CcO complex can potentially induce tumor progression.

§To whom correspondence should be addressed, Narayan G Avadhani, 3800 Spruce Street, Room 189E Vet, Philadelphia, PA 19104, Office: 215-898-8819, Fax: 215-573-6651, ; Email: narayan@vet.upenn.edu

Conflict of Interest: The authors declare no conflict of interest.

Supplementary Information accompanies the paper on the Oncogene website.

Introduction

In keeping with the Warburg hypothesis, proposing aerobic glycolysis as an important factor in tumor growth ([1]), altered mitochondrial function and increased utilization of glucose for energy are hallmarks of many proliferating tumors. A number of studies have shown defective mitochondrial electron transport chain complexes (ETC) in human cancers ([2]–[6]). Epidemiological studies have proposed defective complex I as a biomarker for aggressive thyroid, breast, colon and other cancers ([7]). Similarly mutations in Complex III and complex IV (Cytochrome c oxidase) have been reported in multiple cancers ([3;5;6]). In a majority of these cases, point mutations and deletions in mitochondrial DNA (mtDNA) were shown to be the cause of the defective assembly/function of ETC complexes. However, it still remains unclear if the process of tumorigenesis could be attributed to defects in the ETC complexes.

Loss of mtDNA copy number has been reported in breast, prostate, hepatocellular and lung cancers, and we have shown that partial mtDNA depletion mediates tumorigenesis by activating a Ca^{2+}-Calcineurin dependent retrograde signaling ([8;9]). The onset of this signaling is characterized by loss of mitochondrial membrane potential (Ψm). This results in sustained elevation of $[Ca^{2+}]_c$ followed by activation of Calcineurin (Cn), a Ca^{2+} dependent phosphatase resulting in the activation of a set of stress responsive transcription factors: NFκB (p50:cRel), NFAT, CREB and C/EBPδ ([9]). This signaling also activates an RNA binding protein, hnRNPA2 which acts as a transcription co-activator by binding to the enhanceosome complex through protein-protein interaction ([10;11]). The stress signaling induces expression of wide array of genes with roles in metabolic shift from oxidative phosphorylation to glycolysis, invasiveness, morphological changes and resistance to apoptosis ([8;12]). Lowering of mtDNA copy number induces stress signaling pathway, which reprograms cells to a highly proliferative and tumor producing phenotype and also induces EMT in some epithelial cells. ([13]).

Cytochrome c oxidase (CcO) is a bigenomic enzyme with three of the 13 subunits encoded by mtDNA and remaining 10 subunits encoded by nuclear genes. The nuclear subunits are thought to be important for the assembly or regulation of enzyme activity. Our studies and others' showed that siRNA mediated depletion of the peripheral subunits, IVi1, Vb, and VI not only affects the assembly of intact complex but also the CcO activity, culminating in respiratory dysfunction and disruption of Ψm ([14;15]). Additionally, subunits IVi1 and Vb levels are selectively reduced in hypoxia, myocardial ischemia, alcohol toxicity and other disease conditions ([16]–[20]). Loss of CcO complex also disrupted respirosome super complexes that are thought to play important role in the regulation of electron transport, OXPHOS and attenuation of reactive oxygen species (ROS) production ([21]–[23]).

Here we show that silencing of subunits IVi1 or Vb of CcO induces a mitochondrial retrograde signaling, which largely mimics the signaling we reported in mtDNA depleted cells ([13]). The cells acquired invasiveness and showed loss of contact inhibition generally observed in tumor cells. There was increased expression of marker genes of Ca^{2+}/Calcineurin signaling pathway. As expected, these cells with disrupted CcO complex showed many features of 'Warburg Effect' including increased dependence on glycolysis and invasive behavior in otherwise non-tumorigenic C2C12 skeletal myoblasts. Similarly in

cell lines derived from esophageal and breast cancers, loss of cytochrome oxidase increased invasiveness. Strikingly, in C2C12 cells these changes were reversed by reconstituting subunit IVi1 silenced cells with wild type CcOIVi1 cDNA, thus establishing a novel role of this ETC component in the tumorigenic process.

Results

Disruption of cytochrome c oxidase complex by silencing subunit IVi1 and Vb mRNAs

Fig 1A and B show the relative mRNA and protein levels for CcO subunits IVi1 and Vb in C2C12 cells expressing control (scrambled shRNA) or shRNA for IVi1 and Vb mRNAs, respectively. Cells expressing shRNA for subunit IVi1 (hereafter referred to CcO4KD cells) contained nearly 90% reduced mRNA and protein as compared to cells expressing a scrambled sequence. CcOVb shRNA expressing C2C12 cells (hereafter referred to as CcO5bKD cells) had 65% reduction in Vb mRNA and protein levels (Fig. 1A). C2C12 cells expressing a scrambled shRNA are referred to as control cells. In C2C12 cells, silencing of neither of these subunits had an effect on mRNA levels for other subunits of ETC complexes (Fig S1A). Also, the level of complex IV (CcO) (Fig. 1C) as tested by the Blue Native PAGE was markedly reduced in both CcO4KD and CcO5bKD cells, although the levels of complexes I, II and V did not change. To visualize the effects of CcO knock down on the organization of the respiratory super complexes, we separated digitonin solubilized mitochondrial extracts on 5%–10% gradient blue native gel and probed with antibodies to subunits of either complex I or IV. As seen in Fig 1D, left panel, the slow migrating super complexes containing CcO were significantly depleted in CcOKD cells. On the other hand, when probed with antibody to complex I subunit Grim19 (Fig 1D, right panel), the larger super complexes were absent or reduced in CcOKD cells, while smaller complexes that likely do not contain CcO were unaffected. The CcO enzyme activity was significantly reduced in the knock down cells and was consistent with mRNA levels in both CcO4KD and CcO5bKD cells (Fig 1E). Activities of complex I was marginally lower in CcO4KD cells and complex III activity remained nearly the same in these cells (Fig. 1E).

Figure 2A shows the effects of CcO subunit knock down on mitochondrial morphology. Mitochondria in CcO4KD cells appeared as small fragments and many formed ring like structures with loss of filamentous network (Fig 2A, right panel). Such donut shaped mitochondrial structures have been reported in cells subjected to hypoxia or exposed to mitochondrial toxins ([24]). Mitochondrial network was also affected in CcO5bKD cells although to lesser extent compared to CcO4KD cells (Fig 2A, bottom left). To ascertain that the altered mitochondrial morphology was due to loss of CcO activity, we reconstituted cells by ectopic expression of shRNA resistant subunit IVi1 (CcO4KDshRC4). As shown in Fig 2B, CcO holoenzyme was reconstituted in these cells and the enzyme activity was restored to nearly 80% of control cells (Fig 2C). Reconstitution of cells by ectopic expression of CcOIVi1 cDNA also restored filamentous and network organization of mitochondrial structures (Fig 2B, bottom right).

Bioenergetic stress and metabolic shift in cells with disrupted CcO complex

Oxygen consumption rates (OCR) in control, CcO4KD and CcO5bKD cells were measured using an XF24 flux analyzer (Fig 3A, Left panel). As expected, the basal OCR was lower in both CcO4KD and CcO5bKD cells compared to the control, while in CcO4KDshRC4 cells basal respiration was higher than the parental CcO4KD cells (Fig 3B). The ATP coupled respiration (measured after adding oligomycin) and maximum respiratory capacity (measured following the addition of uncoupler, 2,4 dinitrophenol (DNP)) (Fig. 3C) were markedly reduced in CcO4KD and CcO5bKD cells. In CcO4KDshRC4 cells both ATP coupled respiration and maximum respiratory capacity were significantly recovered compared to CcO4KD cells. Extracellular acidification rate (ECAR) is a measure of glycolytic flux and is significantly higher in CcO4KD cells compared to control cells (Fig 3A, Right panel). In CcO4KDshRC4 cell line the ECAR levels are closer to control levels. Interestingly, in CcO5bKD cells basal ECAR levels was similar to control cells. However, while addition of oligomycin resulted in a significant increase in ECAR in control cells, the effect was comparatively modest in CcO5bKD cells, suggesting that in CcO5bKD cells basal glycolytic flux is closer to its maximum capacity compared to control cells (Fig 3A, Right panel). Knock down of either subunit IVi1 or Vb resulted in about 25–30% increase in DCF fluorescence while it was less than 10% higher in CcO4KDshRC4 cells (Fig 3C) compared to control. Specificity of the signal was verified by treating cells with membrane permeable catalase. Hydrogen peroxide (2.5mM) was used as a positive control (Fig 3C). Total cellular ATP was measured as readout of the bioenergetic status of the cells.

As seen in Fig 4A, cellular ATP levels were 15% to 20% lower in the knockdown cells. However, less than 10% ATP synthesized in CcO4KD and CcO5bKD cells were resistant to oligomycin treatment, while it was ~30% in control cells. In CcO4KDshRC4 cells both total cellular ATP and oligomycin resistant ATP levels were recovered compared to CcO4KD cells (Fig 4A). These results suggest a switch to glycolysis as the main source of ATP in CcOKD cells.

The switch to glycolysis was further supported by results in Fig. 4B showing ~ two fold increase in glycolytic enzyme, hexokinase (HK) and phosphofructokinase (PFK) in CcO4KD cells. In CcO5bKD cells, the increase in HK and PFK activities were about 20–45% over the control. In agreement with these data, glucose uptake in both of these cell lines was >2 fold higher than control cells (Fig. 4C). Wortmannin is an inhibitor of PI3Kinase, while FK506 is an inhibitor of Calcineurin. BAPTA-AM is a Ca^{2+} chelator. All three compounds significantly inhibited glucose uptake by both CcO4KD and CcO5bKD cells. CcO4KDshRC4 cells showed significantly lower glucose uptake than CcO4KD cells. BAPTA-AM reduced glucose uptake further in these cells while Wortmannin and FK506 had only marginal effect (Fig 4C). Glucose uptake was supported by about 2 fold increase in Glut4 mRNA levels in both CcOKD cells (Fig 4D). Interestingly Glut1 levels were largely unaffected in both knock down cells. These results together show that disruption of CcO activity causes a metabolic adaptation to increased glycolysis for ATP production.

Activation of retrograde signaling in CcO disrupted cells

Mitochondrial stress induced by depletion of mtDNA in C2C12 cells was shown to activate a distinctive Ca^{2+}/Cn stress signaling, which induced the expression of many nuclear genes including those involved in tumor progression ([8–10]). Increased Cn activity is an indicator of mtDNA depletion-induced Mt-RS ([8;25–27]). Cn mRNA levels were induced by 2–3 fold in both CcO4KD and CcO5bKD cells, suggesting the activation of Cn pathway (Fig 5A). The Cn mRNA level was markedly reduced in CcO4KDshRC4 cells indicating that the altered Cn expression was due to dysfunctional CcO complex. We observed increased expression of nuclear oncogenes TGF-β and IGF1R in CcO4KD cells (Fig 5A) while the levels were reduced in CcO4KDshRC4 cells. IGF1R was not induced in CcO5bKD cells suggesting subtle difference in the signaling between the CcO4KD and CcO5bKD cells. These results collectively indicate that CcO disruption induces Cn activation and induced expression of several key markers of Mt-RS. To determine the role of Ca^{2+}/Cn in stress signaling mediated by CcO subunit knock down, cells were treated with FK506, an inhibitor of Cn and BAPTA-AM, a Ca^{2+} chelator. As shown in Fig 5B, both BAPTA-AM and FK506, significantly attenuated stress-induced expression of TGFβ, MMP16, and Glut4 genes in CcO4KD cells.

To gain insight on the magnitude of altered gene expression in response to CcO disruption, we performed a whole genome microarray analysis of control and CcO4KD cells. More than 100 genes were up regulated and ~ 35 genes were down regulated in CcO4KD cells compared to control C2C12 cells. We used a cut off of 4-fold changes in our analysis (Fig 6A). Functional cluster analysis showed increase in genes involved in metabolism, cell morphogenesis, ion transport, cell motility and migration (Fig 6A). Interestingly many of these genes have been shown to play important roles in a wide variety of cancers and also that these same genes were shown to be induced in mtDNA depleted C2C12 cells ([8;12]). The list of genes and changes in their expression levels has been presented in Fig S2A. A partial list of genes that are up regulated in response to CcO disruption has been presented in Fig 6B. Induced expression of some of the genes detected in microarray analysis was verified by real time quantitative PCR analysis (Fig 6C). Many genes with recognized roles in tumor development like TGFβ, MMP16, PDK4, and Periostin were all up regulated in CcO4KD cells. Notably, the same genes were also up regulated in CcO5bKD cells although at different levels (Fig 6C). The causal role of CcO dysfunction in the up regulation of these genes was evident by the data in Fig. S2B showing that the levels of expression of these stress target genes were markedly reduced CcO4KDshR4 cells (Fig S2B) that showed functional CcO complex.

Phenotypic Alterations and altered growth characteristics by CcO disruption

The control C2C12 cells become confluent in 3 days, differentiate to myotubes, and die after 3–4 days. CcO4KD cells, on the other hand, showed unusual growth characteristic in that they survive for nearly a week after becoming confluent and lose the ability to differentiate into myotubes (Fig S3A). CcO5bKD cells differentiate to myotubes, but at a much slower rate compared to control. Growth rate was measured by plating equal number of cells and following number of live cells for 3 days. Interestingly, both CcOKD cells grew at significantly slower rates compared to control cells (Fig S3B). Anchorage independent

growth is considered one of the important characteristics of malignantly transformed cells. Soft agar colony formation is a widely used read out for assessing anchorage independent growth of tumor cells. Remarkably, both CcO4KD and CcO5bKD cells formed several distinct visible colonies on soft agar in about 3 weeks (Fig. 7A). The control cells formed fewer colonies under these growth conditions (Fig. 7A). Notably, colony formation with CcO4KD cells was markedly inhibited by PI3-kinase inhibitor, Wortmannin, and IGF1R inhibitor Picropodophyllin, suggesting the requirement of PI3-kinase/IGF1R pathway in mediating this phenotypic transformation (Fig 7B). These results are consistent with our previous reports on Mt-RS induced by partial mtDNA depletion involves activation of PI3-K and induction of IGF1R expression ([28]). The mitochondria targeted antioxidant Mito-CP, on the other hand did not have any significant effect suggesting that the loss of contact inhibition in these cells may not be associated with mitochondrial ROS (Fig. 7A). The quantitation of colony numbers with and without treatments is presented in Fig 7B. Similarly, the number of colonies formed by CcO4KDshRC4 cells was significantly lower than CcO4KD cells (Fig 7A, bottom panel).

Since 3D cultures mimic the *in vivo* tumor environment more closely, we grew these cells in growth factor reduced Matrigel 3D cultures. Fig 7C shows representative colonies from multiple experiments. Phalloidin staining of both CcO4KD and CcO5bKD cells (Fig 7C) showed that the cells formed large multicellular colonies (>30 μm diameter) (Right panel) which survived >3weeks while control cells formed smaller colonies with fewer cells. Previously we showed that Akt1, an oncogenic kinase is activated through retrograde signaling in cells subjected mtDNA depletion ([11]). Immunofluorescence images in Fig 7C (bottom panel) show that Akt1 staining was significantly increased in colonies from both CcO knockdown cell lines. Skeletal myocytes transform into aggressive rhabdomyosarcomas *in vivo.* The tumorispheres formed by CcO4KD and CcO5bKD cells in 3D culture are consistent with the sarcomas suggesting the in vivo tumorigenic potential of these CcOKD cells.

Invasion through basement membrane is a hallmark of highly invasive malignant cells. The ability to invade a matrigel coated membrane is an *in vitro* assay indicative of the *in vivo* metastatic potential of the cells. Fig 7D shows that after 48h of incubation almost no control cells migrated across the membrane, while CcO4KD and CcO5bKD cells migrated through the membrane suggesting their invasive potential. Restoration of CcOIVi1 expression in CcO4KD cells reversed the invasive potential of cells (Fig 7D). These results collectively show that disruption of CcO complex induces Mt-RS which in turn induces changes in growth characteristics, cell morphology and invasive potential. To confirm the generality of this observation, we knocked down CcOIVi1 in multiple human cell lines including esophageal cancer, breast cancer and embryonic kidney cells. The reduction in CcOIVi1 levels in these cell lines varied from 50% to over 80% (Fig S4A). The ratio of extracellular acidification to O_2 consumption rates was significantly higher in knock down cells compared to corresponding control cells indicating increased glycolysis (Fig S4B). Matrigel invasion assay was carried out to determine the invasive potential of CcOKD cells. As seen in figure S4C, cell lines with disrupted CcO level invaded the basement membrane to greater extent than the corresponding control cells. The extent of invasion however varied between cell lines.

Solid tumors often contain severely hypoxic regions ([29]). The relevance of CcO disruption in cellular transformation was assessed in the hypoxic regions of human esophageal tumors and mouse xenograft sections. As seen from Fig 8, in serial sections, the levels of subunits IVi1 and Vb were significantly lower in the core of the tumor mass, which is generally considered as a more hypoxic region, compared to the periphery. Corresponding right panels show the relative diaminobenzidine (DAB) staining, measured as indicated in methods. Fig S5A shows the regions used for measuring DAB intensities. As seen in figure 8, levels of CcOIVi1 and Vb drop significantly towards the interior of the tumor mass compared to the periphery. SDHA, a mitochondrial protein, unaffected by hypoxia was distributed fairly evenly throughout the tumor (Fig S5B). Interestingly, similar pattern of differential CcOIVi1 staining with the intensity the CcOIVi1 staining more prominent in the periphery of the tumor mass with significantly lighter staining in interior regions was observed in mouse xenografts of human esophageal squamous cell carcinoma (Fig S5C, Left panel). The region of lower CcOIVi1 staining corresponded with the region of the same mouse xenograft previously established as hypoxic by pimonidazole staining (Fig S5C) ([30]). There was no significant difference in the distribution of TOM20, a mitochondrial outer membrane protein, not affected by hypoxia (Fig S5C, Right panel). These results suggest that CcO subunit loss has a pathological relevance in tumor progression.

DISCUSSION

Mitochondria participate in multitude of physiological functions including generation of ATP, regulation of Ca^{2+} homeostasis, integration of metabolic pathways, biosynthesis of metabolites, steroid hormone and Urea biosynthesis, and integration and execution of apoptosis. While these functions have been well established for many decades, recent studies suggest additional roles of mitochondria as sensors of environmental and cellular stresses ([31–33]). Disruption of normal mitochondrial function by these stresses and resulting cellular alterations form the basis for a growing list of human diseases, such as mitochondrial myopathies, neurodegenerative diseases, diabetes and many age related diseases ([34]). Although reduced bioenergetic capacity is one of the common outcomes of mitochondrial dysfunction, the mitochondrial stress induced signaling appears to play role in wide range of mitochondrial diseases ([27;34–37]).

The involvement of mitochondria in cancer was first suggested by Warburg who noted that cancer cells have damaged respiration and increased lactate production, a phenomenon referred to as 'aerobic glycolysis' or "Warburg Effect" ([1]). Since then several studies have shown diminished mitochondrial respiration in wide range of cancers, which appears to be a hallmark of many proliferating tumors ([38]). The cause and effect relationship between aerobic glycolysis and tumorigenesis is a topic of intense investigation. Warburg also noted "that injury to respiration should not be so great that the cells are killed, for then no cancer cells could result" ([1]). This suggests that it is not mere depletion of ATP or loss of other essential functions of mitochondria that might have a role in cancer development. Instead, an interesting possibility is signaling initiated by mitochondria under stress could play a role in carcinogenesis ([13;39;40]).

Mitochondrial function can be affected by both genetic and environmental factors. Defects in mtDNA such as mutations, deletions and reduction of copy number- all of which affect the mitochondrial ETC, have been reported in a wide variety of cancers ([3]). Mutations in Complex I subunit ND6 was shown to increase metastatic potential by overproducing reactive oxygen species, while a ND5 mutation promoted tumorigenesis by oxidative stress and Akt activation ([41;42]). Similarly, mitochondrial dysfunction resulting from mutations in nuclear DNA encoded mitochondrial proteins like SDH, FH and IDH, are also strongly associated with specific cancers ([43]–[45]). In these instances, secondary metabolites that accumulate due to absence of the corresponding functional enzyme have been suggested to play a role in metabolic reprogramming of cancer cells ([34]).

Large number of studies have shown defective CI, CII and CIV is many human tumors and mouse xenografts ([34]). Similarly, we and others have shown diminished CcO subunit levels and CcO activity under various pathologies including alcohol toxicity, myocardial disease, cancers, hypoxia, and exposure to environmental toxins ([46]). In the present study using multiple cell lines, we investigated the causative role of CcO dysfunction in metabolic reprogramming and tumor progression by shRNA mediated knockdown of CcO subunits IVi1 and Vb. Our results strikingly show that reduced CcO function and reduced Ψm in C2C12 myoblasts induced a shift in metabolism towards glycolysis, and induced invasive and anchorage independent growth characteristics, similar to tumor cells. Interestingly CcOKD cells grow at a much slower rate compared to control cells suggesting that the stress signaling has a more significant effect on the invasive potential rather than the proliferative phenotype of the cells. These results in effect largely recapitulate the "Warburg effect". Our observation that disruption of CcO activity induces a metabolic shift, and associated changes in nuclear gene expression profile and growth characteristics, has important significance in tumor progression. These are direct effects of CcO dysfunction since reconstitution of activity by expressing the shRNA resistant subunit significantly reversed the signaling cascade and restored the cell growth characteristics.

It is widely believed that Hif-1α which is activated under hypoxia or by increased ROS production is mainly responsible for the adaptive metabolic shift to cope with the reduced O_2 availability ([47;48]). Under the present mitochondrial stress conditions, however, there was no detectable Hif-1α activation (data not shown). Furthermore, our previous studies have shown that the mitochondrial retrograde signaling mediated by the Ca^{2+}/Cn pathway activates IGF1R, PI3-K/Akt1 and hnRNPA2, resulting in a metabolic shift as well as transcriptional reprogramming of gene expression. In support of this observation, the metabolic shift and phenotypic changes were not affected by Mito-CP, a mitochondrial antioxidant, but inhibited by Cn inhibitor and also PI3-K and IGF1R inhibitors suggesting the role of Ca^{2+}/Cn pathway in these CcO disrupted cells.

Subunit IVi1 of CcO is a transmembrane protein which has been suggested to play a role in the enzyme assembly. Subunit Vb, on the other hand is a peripheral protein associated with the complex on the matrix side. Surprisingly, knockdown of both subunits caused disruption and loss of activity though to significantly different level. Consistent with the less severe effect on CcO activity, most of the gene expression and phenotypic changes in CcO5bKD cells are much less severe compared to CcO4KD cells. However, expression of some of the

marker genes did not conform to this rule. We envision two possibilities for this difference in the levels of induction of marker gene expression, invasive properties of cells and the extent of loss of contact inhibition. It is likely that either the threshold of signaling strength in these cells is different or possibly, there is subtle difference in the nature of signaling. It has been shown earlier that some of the component subunits of the ETC including CcO Vb likely have other cytosolic functions ([49]). These could potentially make the phenotypic outcomes more complex to interpret. Similarly, experiments with human cell lines showed that the effect of loss of cytochrome oxidase and resulting mitochondrial dysfunction depends significantly on the cell type and its metabolic phenotype. These possibilities will require further investigation.

Materials and methods

Cell lines and reagents

C2C12 murine skeletal myoblasts (ATCC CRL1772) and HEK 293 human embryonic kidney cells (ATCC CRL3216) were grown in Dulbecco's modified Eagle's medium (Invitrogen) supplemented with 10% fetal bovine serum and 0.1% Penicillin/Streptomycin. Human esophageal squamous cell carcinoma (ESCC) cell line TE11 was a gift from Dr Nishihira who established the cell line and cells were grown in Dulbecco's modified Eagle's medium supplemented by 10% fetal calf serum (Sigma–Aldrich, St. Louis, MO) and 1% penicillin/streptomycin (Invitrogen) as described previously ([50;51]). The earliest frozen stocks of TE11 has been stored at the Cell Culture Core of the University of Pennsylvania. We have propagated cells from frozen stocks of the original vials that were authenticated by short tandem repeat analysis for highly polymorphic microsatellites FES/FPS, vWA31, D22S417, D10S526 and D5S592 as performed by the Cell Culture Core to validate the identity of cells by comparing cells at the earliest stocks we have and those grown >8–12 passages. MCF7 human breast cancer cells (ATCC HTB22) was grown in Eagle's minimal essential medium supplemented with 10% fetal bovine serum, 10μg/ml Insulin and 0.1% Penicillin/Streptomycin. All cell lines have been tested for mycoplasma contamination on a regular basis. Stable C2C12 cell lines expressing shRNA against subunit IVi1 or Vb were generated using pSilencer 2.0 vector as described before ([14]). Stable HEK 293T, TE11 and MCF7 cell lines expressing shRNA against human subunit IVi1 were generated using PLKO.1 lentiviral vector. Selected clones were maintained in a medium containing 1mM pyruvate and 50μg/ml uridine and analyzed for CcO IVi1 and CcO Vb levels by both real-time PCR and Immunoblotting. Primary antibodies used for immunostaining were from Abcam, Cambridge, MA (CcOIVi1, #ab110272; CcO5b, #ab110263; MTCOI, #ab14705; ATPB, #ab14730; Grim19, #ab110240; SDHA, #ab14715) and SantaCruz Biotechnology, Dallas, TX (Tom20, sc-11415). IR conjugated secondary antibodies (IRdye 800, Cat # 926-32210 and IRdye 680, Cat # 926-68021) were from Licor Biotechnology, Lincoln, NE. Fluorescent secondary antibodies (AlexaFluor 488 and AlexaFluor 594) were from Life technologies, Grand island, NY.

Microarray Analysis

Total RNA from control and CcO IVi1 silenced cells was prepared using RNeasy kit (Qiagen) following the manufacturer's instructions. Whole genome expression analysis was

carried out using Affymetrix GeneChip® Mouse Gene 2.0 ST Array. The data were processed by Affymetrix Expression Console using Probeset-Summarize-Engine with default setting of RMA method to calculate the expression level for each probeset of the array (file: rma-gene-full.summary.txt, ([59])). A list of genes (file: zgene_symbol_list.txt. 2x0.01p, ([59])) was then generated, using our own code in Matlab and C-shell script (code: myp.m and mycluster.csh, ([59])), with the criteria that the fold change is more than 2 and the p-value of one-tailed Welch's t-test is less than 0.01. The generated gene list was functionally annotated using DAVID 6.7 (http://david.abcc.ncifcrf.gov/, ([60])) with default setting (file: myfa_table_all.txt.2x0.01p, ([59])). The functional groups of genes were extracted from the annotated file using the corresponding terms (e.g. "signal transduction, ") with our own C-shell script (file: myfa.csh,([59])). Data are deposited in GEO under acquisition number GSE68525.

Statistics

Data are presented as the mean ± s.d. (standard deviation) using n=3 to 5 as indicated in Fig legends. Statistical analyses were performed using Microsoft Excel or Origin software. Differences were determined by unpaired two-tailed Student t test and equality of variance was checked using Ftest. A value of $P < 0.05$ was considered statistically significant.

Supplementary Material

Refer to Web version on PubMed Central for supplementary material.

Acknowledgements

Abbreviations

|	
CcO	Cytochrome c Oxidase
ETC	Electron transport chain
Mt-RS	Mitochondrial retrograde signaling
shRNA	short hairpin RNA
SDHA	Succinate dehydrogenase subunit A
ROS	Reactive oxygen species
Cn	Calcineurin
OCR	Oxygen consumption rate
ECAR	Extracellular acidification rate

DAB   Diaminobenzidine

Reference List

1. Warburg O. On respiratory impairment in cancer cells. Science. 1956 Aug 10; 124(3215):269–270. [PubMed: 13351639]

2. Brandon M, Baldi P, Wallace DC. Mitochondrial mutations in cancer. Oncogene. 2006 Aug 7; 25(34):4647–4662. [PubMed: 16892079]

3. Chatterjee A, Mambo E, Sidransky D. Mitochondrial DNA mutations in human cancer. Oncogene. 2006 Aug 7; 25(34):4663–4674. [PubMed: 16892080]

4. Dakubo GD, Parr RL, Costello LC, Franklin RB, Thayer RE. Altered metabolism and mitochondrial genome in prostate cancer. J Clin Pathol. 2006 Jan; 59(1):10–16. [PubMed: 16394275]

5. Dasgupta S, Hoque MO, Upadhyay S, Sidransky D. Mitochondrial cytochrome B gene mutation promotes tumor growth in bladder cancer. Cancer Res. 2008 Feb 1; 68(3):700–706. doi: 68/3/700 [pii];10.1158/0008-5472.CAN-07-5532 [doi]. [PubMed: 18245469]

6. Gallardo ME, Moreno-Loshuertos R, Lopez C, Casqueiro M, Silva J, Bonilla F, et al. m.6267G>A: a recurrent mutation in the human mitochondrial DNA that reduces cytochrome c oxidase activity and is associated with tumors. Hum Mutat. 2006 Jun; 27(6):575–582. doi: 10.1002/humu.20338 [doi]. [PubMed: 16671096]

7. Fang H, Shen L, Chen T, He J, Ding Z, Wei J, et al. Cancer type-specific modulation of mitochondrial haplogroups in breast, colorectal and thyroid cancer. BMC Cancer. 2010; 10:421. doi: 1471-2407-10-421 [pii];10.1186/1471-2407-10-421 [doi]. Pubmed PMID: PMC2933623. [PubMed: 20704735]

8. Amuthan G, Biswas G, Ananadatheerthavarada HK, Vijayasarathy C, Shephard HM, Avadhani NG. Mitochondrial stress-induced calcium signaling, phenotypic changes and invasive behavior in human lung carcinoma A549 cells. Oncogene. 2002 Nov 7; 21(51):7839–7849. [PubMed: 12420221]

9. Biswas G, Adebanjo OA, Freedman BD, Anandatheerthavarada HK, Vijayasarathy C, Zaidi M, et al. Retrograde Ca2+ signaling in C2C12 skeletal myocytes in response to mitochondrial genetic and metabolic stress: a novel mode of inter-organelle crosstalk. EMBO J. 1999 Feb 1; 18(3):522–533. [PubMed: 9927412]

10. Guha M, Pan H, Fang JK, Avadhani NG. Heterogeneous nuclear ribonucleoprotein A2 is a common transcriptional coactivator in the nuclear transcription response to mitochondrial respiratory stress. Mol Biol Cell. 2009 Sep; 20(18):4107–4119. doi: E09-04-0296 [pii];10.1091/mbc.E09-04-0296 [doi]. Pubmed PMID: PMC2743628. [PubMed: 19641020]

11. Guha M, Fang JK, Monks R, Birnbaum MJ, Avadhani NG. Activation of Akt is essential for the propagation of mitochondrial respiratory stress signaling and activation of the transcriptional coactivator heterogeneous ribonucleoprotein A2. Mol Biol Cell. 2010 Oct 15; 21(20):3578–3589. doi: E10-03-0192 [pii];10.1091/mbc.E10-03-0192 [doi]. Pubmed PMID: PMC2954122. [PubMed: 20719961]

12. Biswas G, Tang W, Sondheimer N, Guha M, Bansal S, Avadhani NG. A distinctive physiological role for IkappaBbeta in the propagation of mitochondrial respiratory stress signaling. J Biol Chem. 2008 May 2; 283(18):12586–12594. doi: M710481200 [pii];10.1074/jbc.M710481200 [doi]. Pubmed PMID: PMC2335355. [PubMed: 18272519]

13. Guha M, Srinivasan S, Ruthel G, Kashina AK, Carstens RP, Mendoza A, et al. Mitochondrial retrograde signaling induces epithelial-mesenchymal transition and generates breast cancer stem cells. Oncogene. 2013 Nov 4. doi: onc2013467 [pii];10.1038/onc.2013.467 [doi].

14. Galati D, Srinivasan S, Raza H, Prabu SK, Hardy M, Chandran K, et al. Role of nuclear-encoded subunit Vb in the assembly and stability of cytochrome c oxidase complex: implications in mitochondrial dysfunction and ROS production. Biochem J. 2009 Jun 15; 420(3):439–449. doi: BJ20090214 [pii];10.1042/BJ20090214 [doi]. Pubmed PMID: PMC2735414. [PubMed: 19338496]

15. Li Y, Park JS, Deng JH, Bai Y. Cytochrome c oxidase subunit IV is essential for assembly and respiratory function of the enzyme complex. J Bioenerg Biomembr. 2006 Dec; 38(5-6):283–291. doi: 10.1007/s10863-006-9052-z [doi]. Pubmed PMID: PMC1885940. [PubMed: 17091399]

16. Bansal S, Srinivasan S, Anandasadagopan S, Chowdhury AR, Selvaraj V, Kalyanaraman B, et al. Additive effects of mitochondrion-targeted cytochrome CYP2E1 and alcohol toxicity on cytochrome c oxidase function and stability of respirosome complexes. J Biol Chem. 2012 May 4; 287(19):15284–15297. doi: M111.314062 [pii];10.1074/jbc.M111.314062 [doi]. Pubmed PMID: PMC3346148. [PubMed: 22396533]

17. Prabu SK, Anandatheerthavarada HK, Raza H, Srinivasan S, Spear JF, Avadhani NG. Protein kinase A-mediated phosphorylation modulates cytochrome c oxidase function and augments hypoxia and myocardial ischemia-related injury. J Biol Chem. 2006 Jan 27; 281(4):2061–2070. doi: M507741200 [pii];10.1074/jbc.M507741200 [doi]. [PubMed: 16303765]

18. Fang JK, Prabu SK, Sepuri NB, Raza H, Anandatheerthavarada HK, Galati D, et al. Site specific phosphorylation of cytochrome c oxidase subunits I, IVi1 and Vb in rabbit hearts subjected to ischemia/reperfusion. FEBS Lett. 2007 Apr 3; 581(7):1302–1310. doi: S0014-5793(07)00208-6 [pii];10.1016/j.febslet.2007.02.042 [doi]. Pubmed PMID: PMC1995084. [PubMed: 17349628]

19. Sayen MR, Gustafsson AB, Sussman MA, Molkentin JD, Gottlieb RA. Calcineurin transgenic mice have mitochondrial dysfunction and elevated superoxide production. Am J Physiol Cell Physiol. 2003 Feb; 284(2):C562–C570. doi: 10.1152/ajpcell.00336.2002 [doi];00336.2002 [pii]. [PubMed: 12397029]

20. Fukuda R, Zhang H, Kim JW, Shimoda L, Dang CV, Semenza GL. HIF-1 regulates cytochrome oxidase subunits to optimize efficiency of respiration in hypoxic cells. Cell. 2007 Apr 6; 129(1): 111–122. doi: S0092-8674(07)00307-8 [pii];10.1016/j.cell.2007.01.047 [doi]. [PubMed: 17418790]

21. Schafer E, Seelert H, Reifschneider NH, Krause F, Dencher NA, Vonck J. Architecture of active mammalian respiratory chain supercomplexes. J Biol Chem. 2006 Jun 2; 281(22):15370–15375. doi: M513525200 [pii];10.1074/jbc.M513525200 [doi]. [PubMed: 16551638]

22. Vonck J, Schafer E. Supramolecular organization of protein complexes in the mitochondrial inner membrane. Biochim Biophys Acta. 2009 Jan; 1793(1):117–124. doi: S0167-4889(08)00201-2 [pii];10.1016/j.bbamcr.2008.05.019 [doi]. [PubMed: 18573282]

23. Acin-Perez R, Fernandez-Silva P, Peleato ML, Perez-Martos A, Enriquez JA. Respiratory active mitochondrial supercomplexes. Mol Cell. 2008 Nov 21; 32(4):529–539. doi: S1097-2765(08)00762-4 [pii];10.1016/j.molcel.2008.10.021 [doi]. [PubMed: 19026783]

24. Liu X, Hajnoczky G. Altered fusion dynamics underlie unique morphological changes in mitochondria during hypoxia-reoxygenation stress. Cell Death Differ. 2011 Oct; 18(10):1561–1572. doi: cdd201113 [pii];10.1038/cdd.2011.13 [doi]. Pubmed PMID: PMC3172112. [PubMed: 21372848]

25. Biswas G, Anandatheerthavarada HK, Zaidi M, Avadhani NG. Mitochondria to nucleus stress signaling: a distinctive mechanism of NFkappaB/Rel activation through calcineurin-mediated inactivation of IkappaBbeta. J Cell Biol. 2003 May 12; 161(3):507–519. doi: 10.1083/jcb. 200211104 [doi];jcb.200211104 [pii]. Pubmed PMID: PMC2172940. [PubMed: 12732617]

26. Biswas G, Guha M, Avadhani NG. Mitochondria-to-nucleus stress signaling in mammalian cells: nature of nuclear gene targets, transcription regulation, and induced resistance to apoptosis. Gene. 2005 Jul 18.354:132–139. [PubMed: 15978749]

27. Butow RA, Avadhani NG. Mitochondrial signaling: the retrograde response. Mol Cell. 2004 Apr 9; 14(1):1–15. [PubMed: 15068799]

28. Guha M, Srinivasan S, Biswas G, Avadhani NG. Activation of a novel calcineurin-mediated insulin-like growth factor-1 receptor pathway, altered metabolism, and tumor cell invasion in cells subjected to mitochondrial respiratory stress. J Biol Chem. 2007 May 11; 282(19):14536–14546. doi: M611693200 [pii];10.1074/jbc.M611693200 [doi]. Pubmed PMID: PMC3800738. [PubMed: 17355970]

29. Wilson WR, Hay MP. Targeting hypoxia in cancer therapy. Nat Rev Cancer. 2011 Jun; 11(6):393–410. doi: nrc3064 [pii];10.1038/nrc3064 [doi]. [PubMed: 21606941]

30. Natsuizaka M, Naganuma S, Kagawa S, Ohashi S, Ahmadi A, Subramanian H, et al. Hypoxia induces IGFBP3 in esophageal squamous cancer cells through HIF-1alpha-mediated mRNA

transcription and continuous protein synthesis. FASEB J. 2012 Jun; 26(6):2620–2630. doi: fj-11-198598 [pii];10.1096/fj.11-198598 [doi]. Pubmed PMID: PMC3360153. [PubMed: 22415309]

31. Guzy RD, Schumacker PT. Oxygen sensing by mitochondria at complex III: the paradox of increased reactive oxygen species during hypoxia. Exp Physiol. 2006 Sep; 91(5):807–819. doi: expphysiol.2006.033506 [pii];10.1113/expphysiol.2006.033506 [doi]. [PubMed: 16857720]

32. Vannuvel K, Renard P, Raes M, Arnould T. Functional and morphological impact of ER stress on mitochondria. J Cell Physiol. 2013 Sep; 228(9):1802–1818. doi: 10.1002/jcp.24360 [doi]. [PubMed: 23629871]

33. Rainbolt TK, Saunders JM, Wiseman RL. Stress-responsive regulation of mitochondria through the ER unfolded protein response. Trends Endocrinol Metab. 2014 Oct; 25(10):528–537. doi: S1043-2760(14)00106-4 [pii];10.1016/j.tem.2014.06.007 [doi]. [PubMed: 25048297]

34. Wallace DC. Mitochondria and cancer. Nat Rev Cancer. 2012 Oct; 12(10):685–698. doi: nrc3365 [pii];10.1038/nrc3365 [doi]. [PubMed: 23001348]

35. Frezza C. The role of mitochondria in the oncogenic signal transduction. Int J Biochem Cell Biol. 2014 Mar.48:11–17. doi: S1357-2725(13)00382-8 [pii];10.1016/j.biocel.2013.12.013 [doi]. [PubMed: 24397955]

36. Moro L, Arbini AA, Yao JL, di Sant'Agnese PA, Marra E, Greco M. Mitochondrial DNA depletion in prostate epithelial cells promotes anoikis resistance and invasion through activation of PI3K/ Akt2. Cell Death Differ. 2009 Apr; 16(4):571–583. doi: cdd2008178 [pii];10.1038/cdd.2008.178 [doi]. [PubMed: 19079138]

37. Wallace DC. Mitochondrial DNA mutations in diseases of energy metabolism. J Bioenerg Biomembr. 1994 Jun; 26(3):241–250. [PubMed: 8077179]

38. Pelicano H, Xu RH, Du M, Feng L, Sasaki R, Carew JS, et al. Mitochondrial respiration defects in cancer cells cause activation of Akt survival pathway through a redox-mediated mechanism. J Cell Biol. 2006 Dec 18; 175(6):913–923. [PubMed: 17158952]

39. Amuthan G, Biswas G, Zhang SY, Klein-Szanto A, Vijayasarathy C, Avadhani NG. Mitochondria-to-nucleus stress signaling induces phenotypic changes, tumor progression and cell invasion. EMBO J. 2001 Apr 17; 20(8):1910–1920. [PubMed: 11296224]

40. Guha M, Avadhani NG. Mitochondrial retrograde signaling at the crossroads of tumor bioenergetics, genetics and epigenetics. Mitochondrion. 2013 Nov; 13(6):577–591. doi: S1567-7249(13)00240-7 [pii];10.1016/j.mito.2013.08.007 [doi]. Pubmed PMID: PMC3832239. [PubMed: 24004957]

41. Ishikawa K, Takenaga K, Akimoto M, Koshikawa N, Yamaguchi A, Imanishi H, et al. ROS-generating mitochondrial DNA mutations can regulate tumor cell metastasis. Science. 2008 May 2; 320(5876):661–664. doi: 1156906 [pii];10.1126/science.1156906 [doi]. [PubMed: 18388260]

42. Sharma LK, Fang H, Liu J, Vartak R, Deng J, Bai Y. Mitochondrial respiratory complex I dysfunction promotes tumorigenesis through ROS alteration and AKT activation. Hum Mol Genet. 2011 Dec 1; 20(23):4605–4616. doi: ddr395 [pii];10.1093/hmg/ddr395 [doi]. Pubmed PMID: PMC3209831. [PubMed: 21890492]

43. Bardella C, Pollard PJ, Tomlinson I. SDH mutations in cancer. Biochim Biophys Acta. 2011 Nov; 1807(11):1432–1443. doi: S0005-2728(11)00162-9 [pii];10.1016/j.bbabio.2011.07.003 [doi]. [PubMed: 21771581]

44. Krell D, Assoku M, Galloway M, Mulholland P, Tomlinson I, Bardella C. Screen for IDH1, IDH2, IDH3, D2HGDH and L2HGDH mutations in glioblastoma. PLoS One. 2011; 6(5):e19868. doi: 10.1371/journal.pone.0019868 [doi];PONE-D-11-03045 [pii]. Pubmed PMID: PMC3100313. [PubMed: 21625441]

45. Picaud S, Kavanagh KL, Yue WW, Lee WH, Muller-Knapp S, Gileadi O, et al. Structural basis of fumarate hydratase deficiency. J Inherit Metab Dis. 2011 Jun; 34(3):671–676. doi: 10.1007/ s10545-011-9294-8 [doi]. Pubmed PMID: PMC3109261. [PubMed: 21445611]

46. Srinivasan S, Avadhani NG. Cytochrome c oxidase dysfunction in oxidative stress. Free Radic Biol Med. 2012 Sep 15; 53(6):1252–1263. doi: S0891-5849(12)00416-9 [pii];10.1016/j.freeradbiomed. 2012.07.021 [doi]. Pubmed PMID: PMC3436951. [PubMed: 22841758]

47. Semenza GL, Roth PH, Fang HM, Wang GL. Transcriptional regulation of genes encoding glycolytic enzymes by hypoxia-inducible factor 1. J Biol Chem. 1994 Sep 23; 269(38):23757–23763. [PubMed: 8089148]

48. Chandel NS, McClintock DS, Feliciano CE, Wood TM, Melendez JA, Rodriguez AM, et al. Reactive oxygen species generated at mitochondrial complex III stabilize hypoxia-inducible factor-1alpha during hypoxia: a mechanism of O2 sensing. J Biol Chem. 2000 Aug 18; 275(33): 25130–25138. doi: 10.1074/jbc.M001914200 [doi];M001914200 [pii]. [PubMed: 10833514]

49. Chen ZX, Pervaiz S. Involvement of cytochrome c oxidase subunits Va and Vb in the regulation of cancer cell metabolism by Bcl-2. Cell Death Differ. 2010 Mar; 17(3):408–420. doi: cdd2009132 [pii];10.1038/cdd.2009.132 [doi]. [PubMed: 19834492]

50. Nakagawa H, Zukerberg L, Togawa K, Meltzer SJ, Nishihara T, Rustgi AK. Human cyclin D1 oncogene and esophageal squamous cell carcinoma. Cancer. 1995 Aug 15; 76(4):541–549. [PubMed: 8625145]

51. Nishihira T, Hashimoto Y, Katayama M, Mori S, Kuroki T. Molecular and cellular features of esophageal cancer cells. J Cancer Res Clin Oncol. 1993; 119(8):441–449. [PubMed: 8509434]

52. Srinivasan S, Spear J, Chandran K, Joseph J, Kalyanaraman B, Avadhani NG. Oxidative stress induced mitochondrial protein kinase A mediates cytochrome c oxidase dysfunction. PLoS One. 2013; 8(10):e77129. doi: 10.1371/journal.pone.0077129 [doi];PONE-D-13-24168 [pii]. Pubmed PMID: PMC3795003. [PubMed: 24130844]

53. Lowry OH, ROSEBROUGH NJ, FARR AL, RANDALL RJ. Protein measurement with the Folin phenol reagent. J Biol Chem. 1951 Nov; 193(1):265–275. [PubMed: 14907713]

54. Nijtmans LG, Taanman JW, Muijsers AO, Speijer D, Van den Bogert C. Assembly of cytochrome-c oxidase in cultured human cells. Eur J Biochem. 1998 Jun 1; 254(2):389–394. [PubMed: 9660196]

55. Miccoli L, Oudard S, Sureau F, Poirson F, Dutrillaux B, Poupon MF. Intracellular pH governs the subcellular distribution of hexokinase in a glioma cell line. Biochem J. 1996 Feb 1; 313(Pt 3):957–962. Pubmed PMID: PMC1217004. [PubMed: 8611181]

56. Devin A, Nogueira V, Leverve X, Guerin B, Rigoulet M. Allosteric activation of pyruvate kinase via NAD+ in rat liver cells. Eur J Biochem. 2001 Jul; 268(14):3943–3949. doi: ejb2306 [pii]. [PubMed: 11453987]

57. Frevert EU, Kahn BB. Differential effects of constitutively active phosphatidylinositol 3-kinase on glucose transport, glycogen synthase activity, and DNA synthesis in 3T3-L1 adipocytes. Mol Cell Biol. 1997 Jan; 17(1):190–198. Pubmed PMID: PMC231743. [PubMed: 8972199]

58. Scholl C, Frohling S, Dunn IF, Schinzel AC, Barbie DA, Kim SY, et al. Synthetic lethal interaction between oncogenic KRAS dependency and STK33 suppression in human cancer cells. Cell. 2009 May 29; 137(5):821–834. doi: S0092-8674(09)00316-X [pii];10.1016/j.cell.2009.03.017 [doi]. [PubMed: 19490892]

59. http://code.vet.upenn.edu/download/CcOdefect/. 8-21-2014. Ref Type: Online Source

60. Huang, dW; Sherman, BT.; Lempicki, RA. Systematic and integrative analysis of large gene lists using DAVID bioinformatics resources. Nat Protoc. 2009; 4(1):44–57. doi: nprot.2008.211 [pii]; 10.1038/nprot.2008.211 [doi]. [PubMed: 19131956]
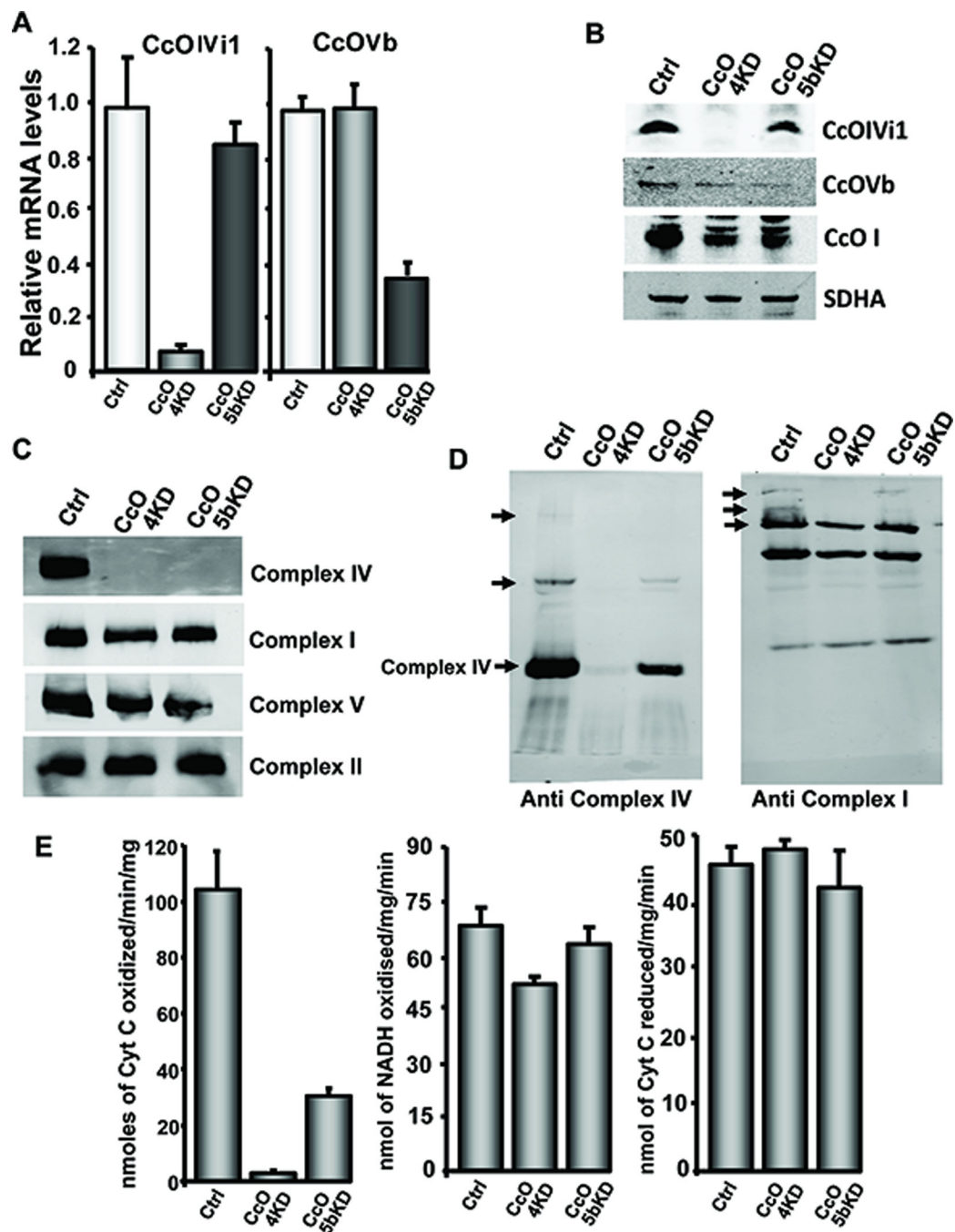
Figure 1.
Knockdown of CcO IVi1 and Vb disrupts complex IV assembly and activity: A) Relative mRNA and B) protein levels for CcO subunits IVi1 and Vb in control (Ctrl), CcO4KD and CcO5bKD cells. Beta actin (A) and SDHA (B) were used as endogenous and loading controls. C&D) Blue native gel pattern of mitochondrial electron transport chain complexes in IVi1 and Vb knockdown cells as described in Materials and methods available online in Supplemental information. Sodium dodecyl maltoside solubilized mitochondria were separated to visualize monomeric complexes (C) and Digitonin solubilized mitochondria

were used for separating super complexes (D). SDHA was used as loading control. E) Enzyme activities of complex IV (left), complex I (middle) and complex III (right) in CcO knockdown cell lines.
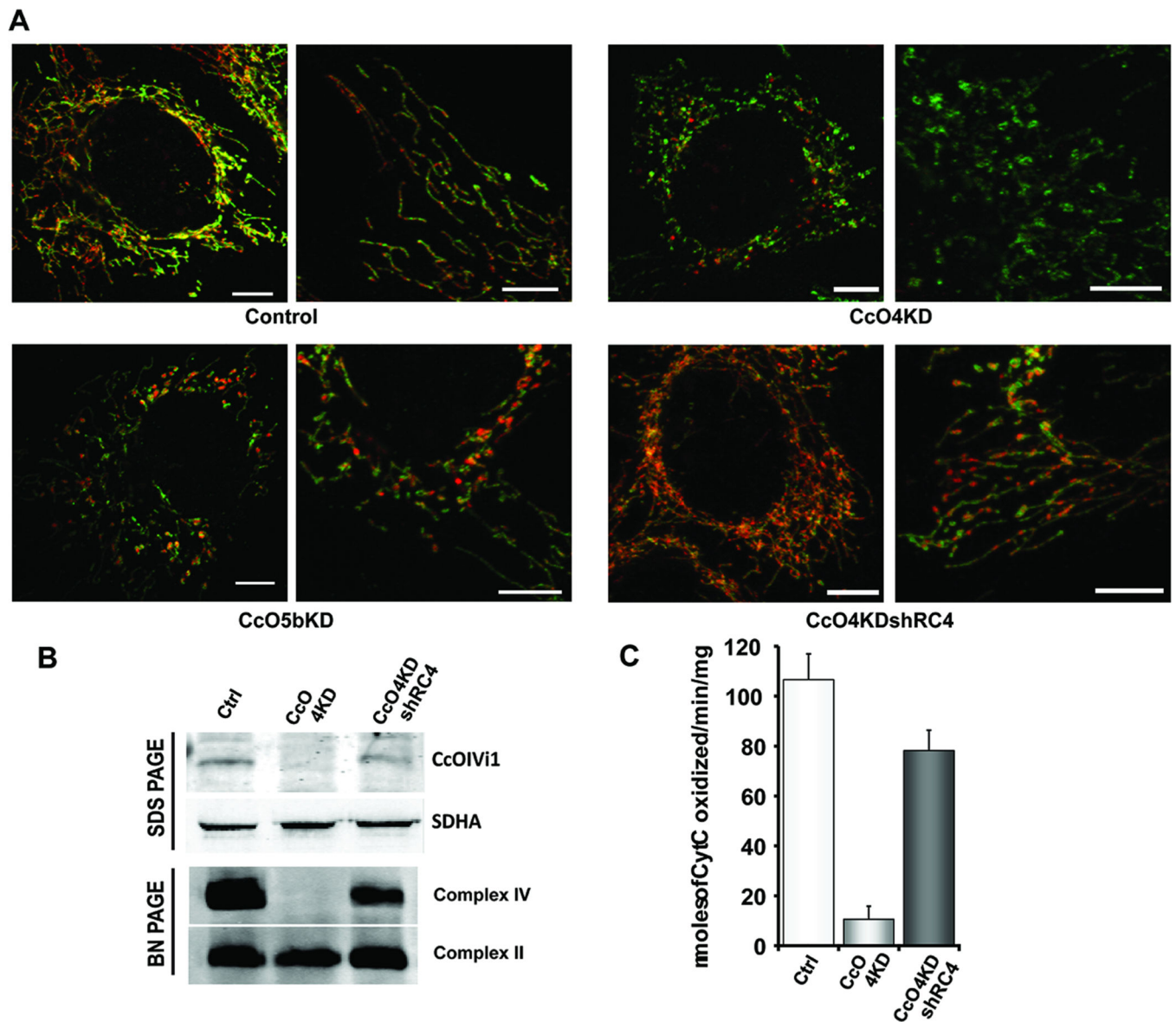
Figure 2.
Knockdown of CcO IVi1 and Vb disrupts mitochondrial morphology. A) Confocal microscopy showing mitochondrial morphology in control, CcO4KD, CcO5bKD and CcO4KDshRC4 cells as described in Materials and methods available online in Supplemental information. Cells were stained with antibodies to Complex V, ATPB (green) and CcO IVi1 (red). Scale: 2.5µm. B) SDS PAGE (top panel) and blue native PAGE (bottom panel) immunoblots showing expression of shRNA resistant CcOIVi1 subunit and reconstitution of complex IV in CcO4KD cells. C) Recovery of cytochrome oxidase enzyme activity in CcO4KDshRC4 cells.
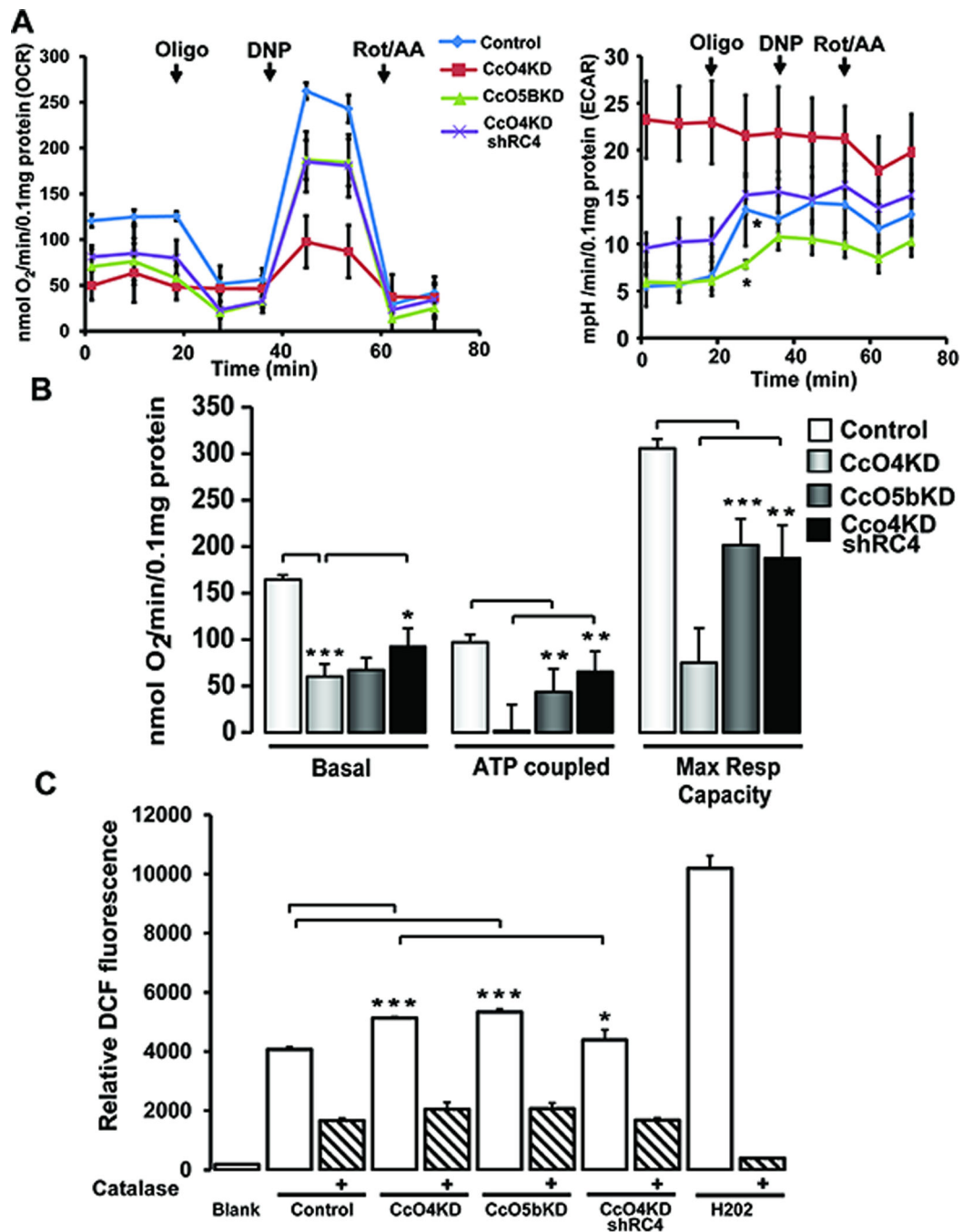
Figure 3.
Altered bioenergetics in CcO IVi1 and Vb knockdown cells: A) Respiratory profile (Left panel) and Extracellular acidification rate (Right panel) of control, CcO4KD, CcO5bKD and CcO4KDshRC4 cells Vb knockdown cells under basal, and after Oligomycin (Oligo, 2µg/ml), 2,4 dinitrophenol (DNP, 100µM) and Rotenone/Antimycin (Rot/AA, 1µM each) addition, measured in a Seahorse respirometer as described in Materials and methods available online in Supplemental information. At the end of measurement, protein was estimated by Lowry's method and the OCR values were normalized to 0.1mg protein.

*=between control and CcO5bKD B) ATP coupled respiration and Maximum respiratory capacity in the four cell lines. ATP coupled respiration was calculated by subtracting OCR values after addition of Oligomycin from basal OCR. Maximum respiratory capacity was calculated by subtracting OCR values after addition of Rotenone from OCR values obtained after adding 2,4 Dinitrophenol C) Measurement of ROS by DCF oxidation in control, CcO4KD, CcO5bKD and CcO4KDshRC4 cells. Cells $1X10^6$ were incubated with $1\mu M$ DCFHDA at 37°C for 20 min. For catalase treatment, 1U of Polyethylene glycol conjugated Catalase was added 10 min prior to DCFHDA addition as described in Materials and methods available online in Supplemental information. H_2O_2 (2.5mM) was used as positive control. *P 0.05; **P 0.01; n=3.
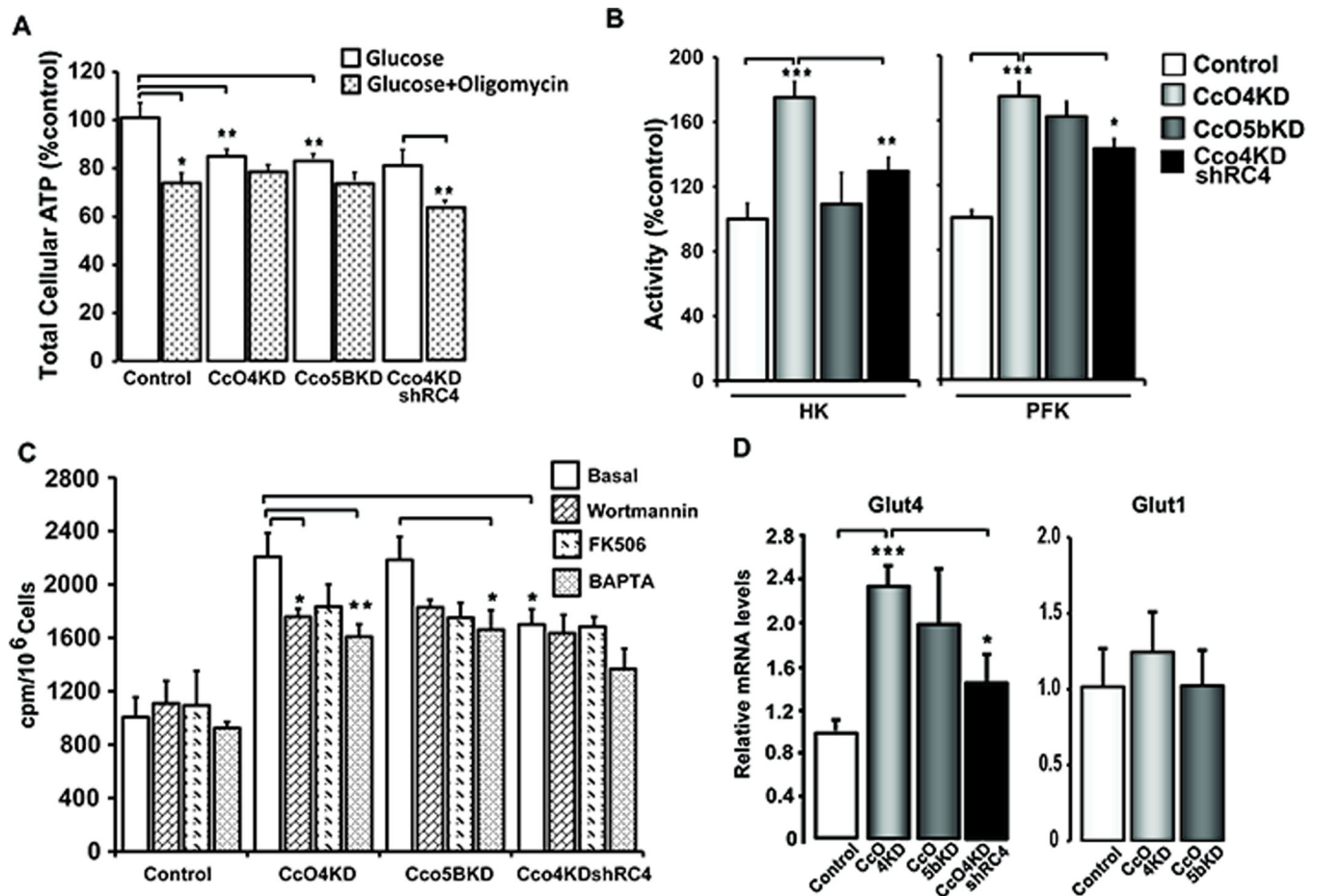
Figure 4.
Knockdown of CcO subunits increases glucose uptake and glycolytic enzymes. A) Total cellular ATP in control and knockdown cells with or without added Oligomycin. Cells grown in 96 well plates were treated with either DMSO or 2μg/ml oligomycin for 4h before ATP estimation. ATP was measured using a Bioluminescence kit as described in Materials and methods available online in Supplemental information. The total cellular ATP of control cells was considered as 100%. B) Activities of glycolytic enzymes in total cell lysates from control, CcO knockdown and CcO4KDshRC4 cells. Hexokinase (HK) and Phosphofructokinase (PFK) activities were measured using 50 μg of protein for each point as described in Materials and methods available online in Supplemental information. The activity of control samples was considered as 100% activity for each enzyme assay. C) 2-deoxy glucose uptake measured in control, knockdown and CcO4KDshRC4 cells as described in Materials and methods available online in Supplemental information. Cells (1×10^5) were plated in 12 well culture dishes and treated with or without Wortmannin (1μM) or FK506 (0.5 μM) or BAPTA (20μM) for 24h. D) Relative mRNA level for Glut 4 and Glut 1 glucose transporters as measured by real time quantitative PCR. Beta actin was used as endogenous control for normalization. *P 0.05; **P 0.01; ***P 0.001; n=3.
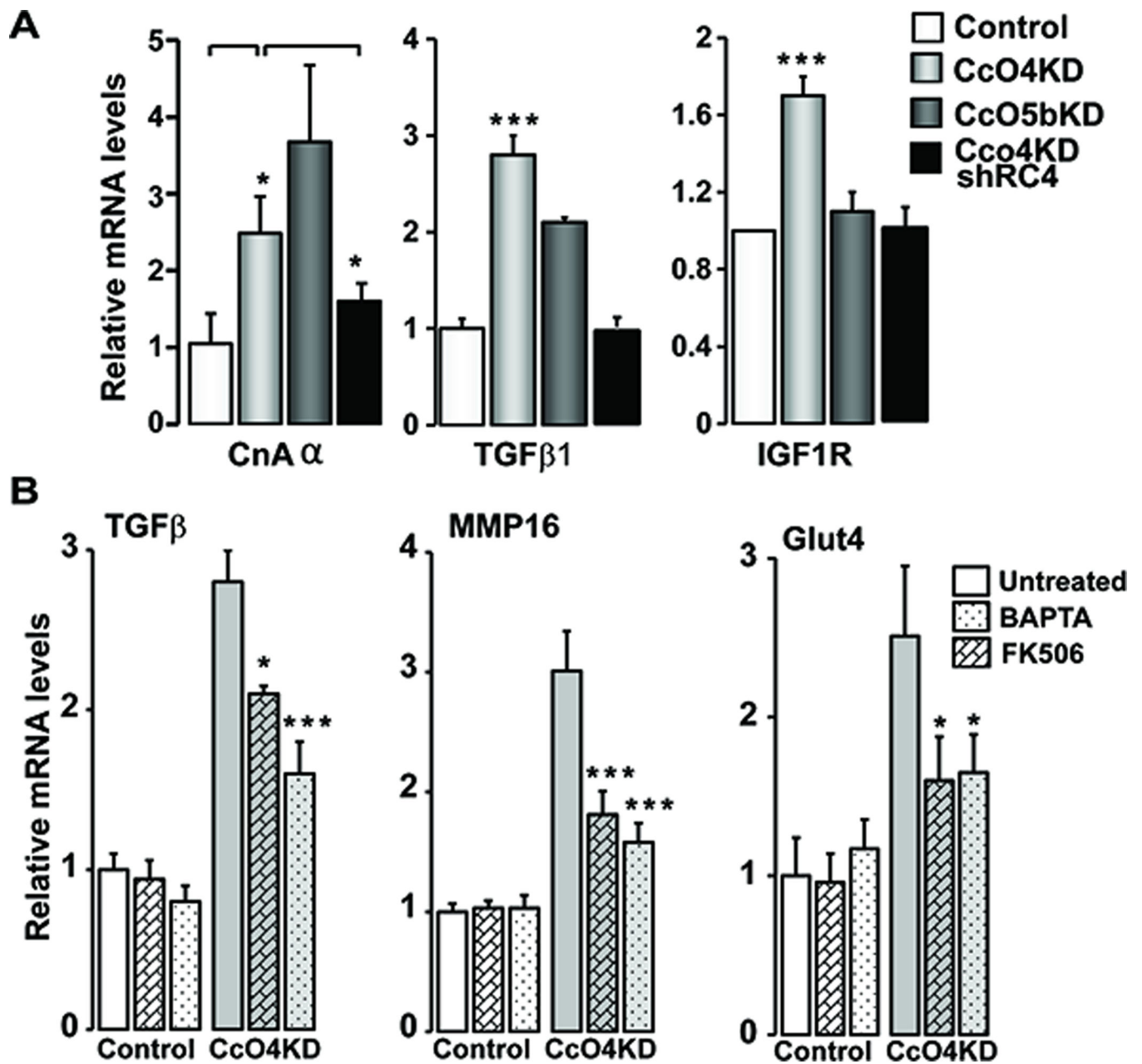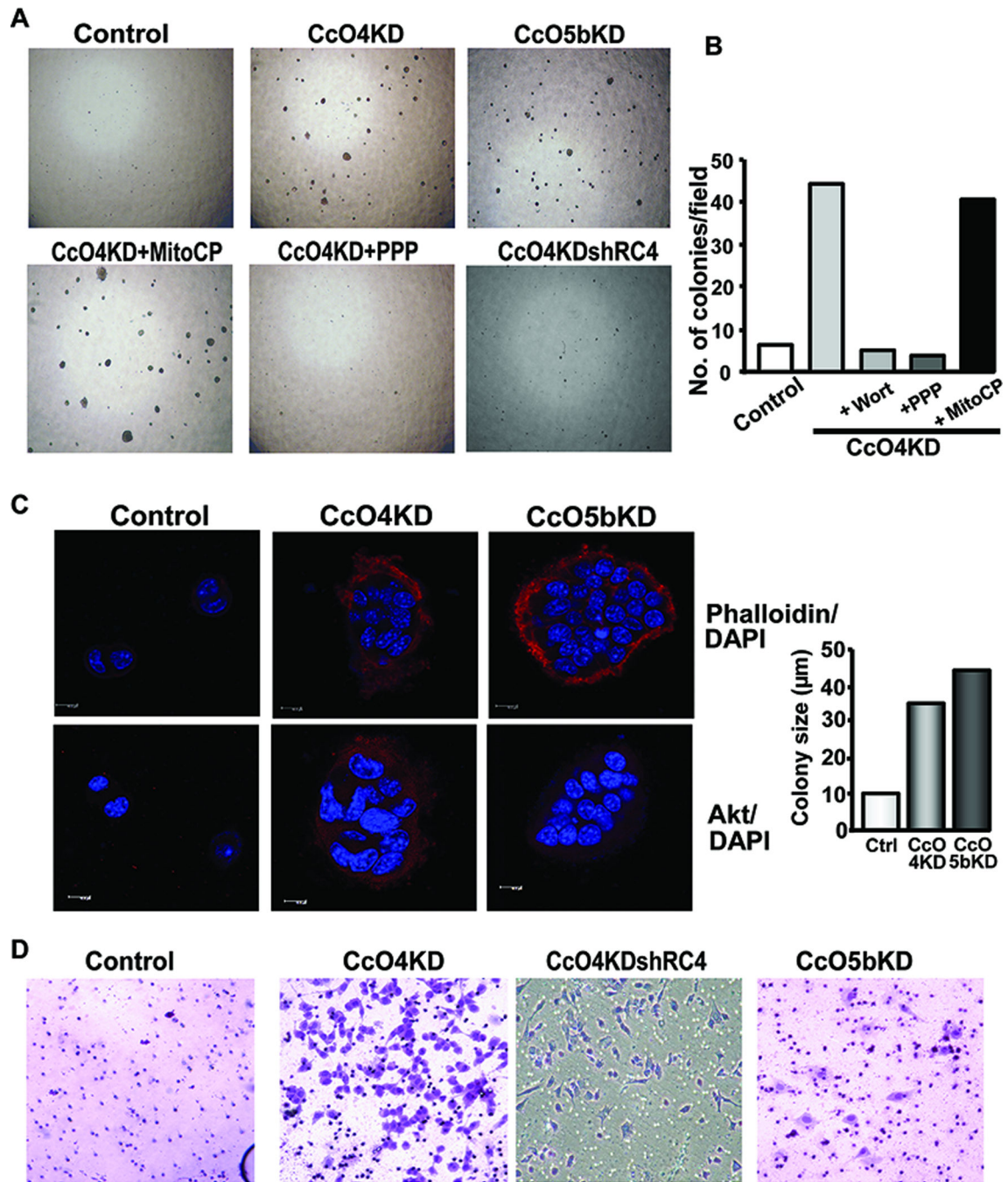
Figure 5.
Activation of mitochondrial retrograde signaling in CcO knockdown cells: A) Relative mRNA levels of MtRS marker genes Calcineurin Aα (CnAα), TGFβ1 and IGF1R (n=3) in control, CcO IVi1 and Vb knockdown and CcO4KDshRC4 cells. B) Effect of FK506 (0.5μM) and BAPTA (20μM) on induction of stress target genes in CcO4KD cells. The cells were treated for 24h with indicated compounds before analysis. Beta actin was used as endogenous control. *P 0.05; ***P 0.001; n=3.
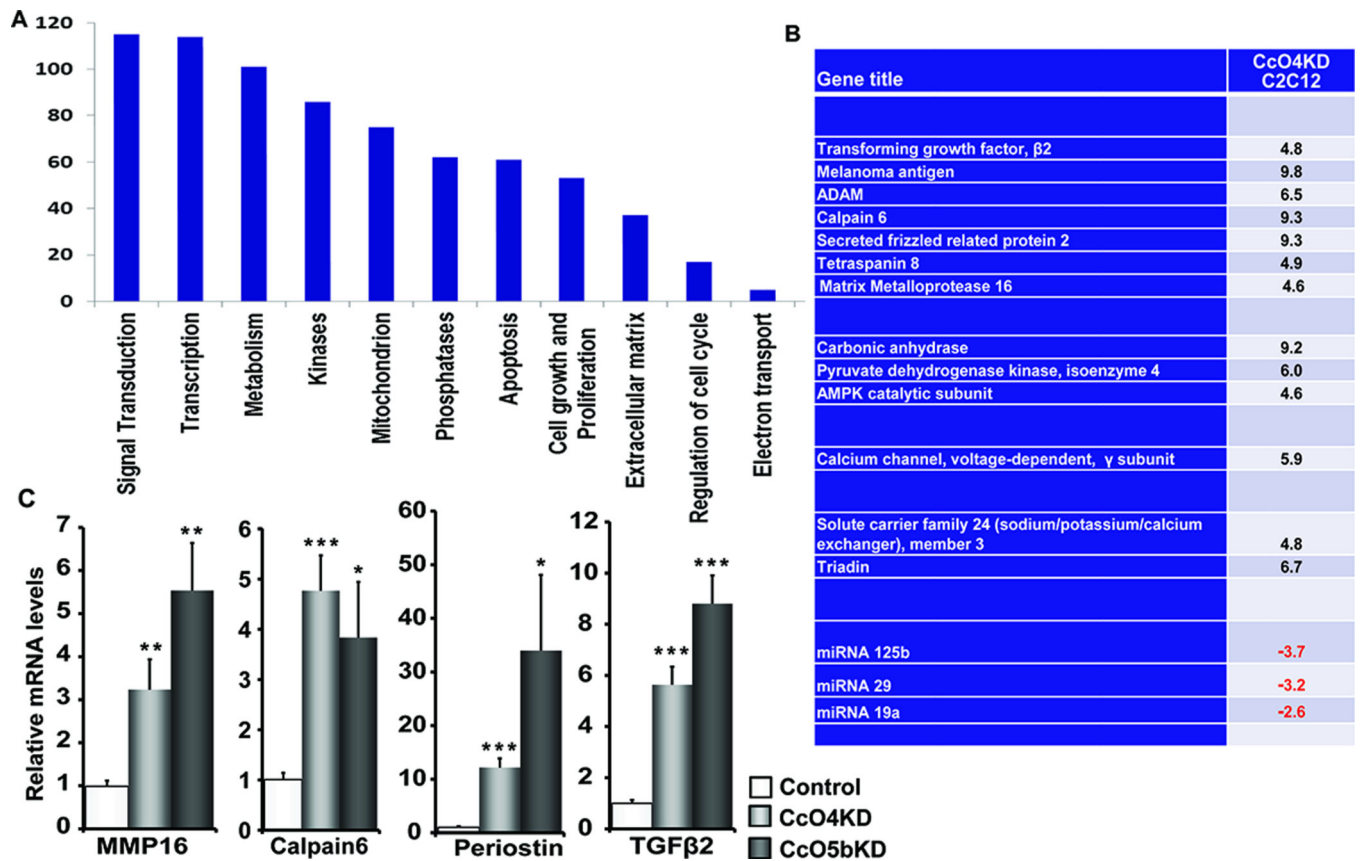
Figure 6.
CcO knockdown induces expression of several oncogenic genes: A) Functional groups of genes up regulated in CcO IVi1 knockdown cells compared to control cells. Whole genome expression analysis was performed using Mouse Affymetrix 2.0 gene array. B) List of genes known to play significant role in tumor growth. C) Relative mRNA levels of genes identified in genome array analysis in Control, CcO4KD and CcO5bKD cells. The mRNA levels were measured by real time PCR as described in Methods *P 0.05; ***P 0.001 (n=3).

Figure 7.
CcO knockdown cells acquire invasive phenotype: A) Soft agar assay for anchorage independent growth of Control, CcO4KD, CcO5bKD cells and CcO4KD cells treated with 1µM MitoCP, 2.5µM Picropodophyllin, or expressing shRNA resistant CcO4i1 (CcO4KDshR4) as described in Materials and methods available online in Supplemental information. Cells (3000) were plated in 0.3% agarose supplemented with complete DMEM medium. Colonies were allowed to grow for 3 weeks and imaged using a bright field microscope. B) Effect of Wortmannin (Wort), PicropodophyllinPPP and MitoCP on soft agar

colony formation of CcO IVi1 knockdown cells. C) Confocal images of Phalloidin and DAPI stained colonies of control and CcO knockdown cells grown under 3D culture conditions in 2% matrigel. The right panel shows quantitation of colony size, measured as diameter of the colony in μm. D) Matrigel invasion pattern of Control, CcO knockdown cells and CcO4KDshR4 cells 24h after plating as described in Materials and methods available online in Supplemental information. Cells were stained with Hematoxylin and Eosin and imaged by bright field microscopy.
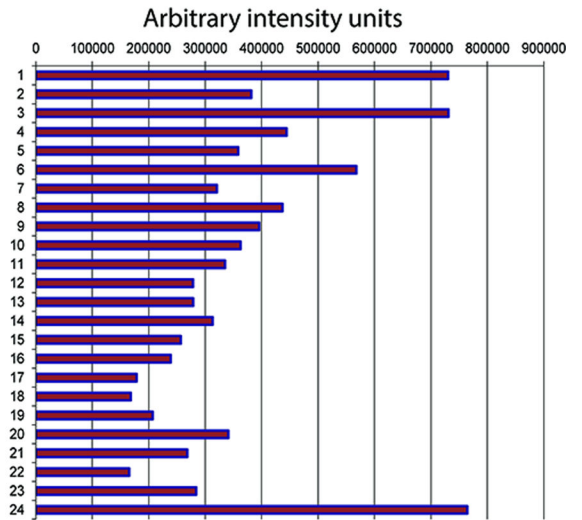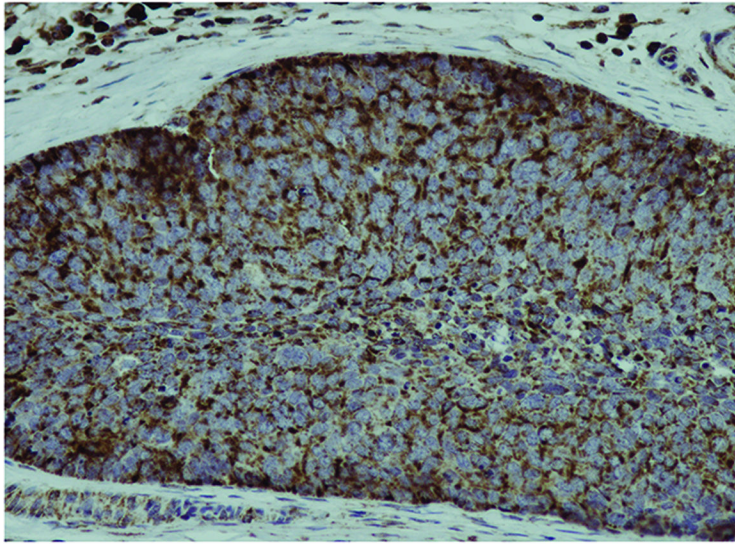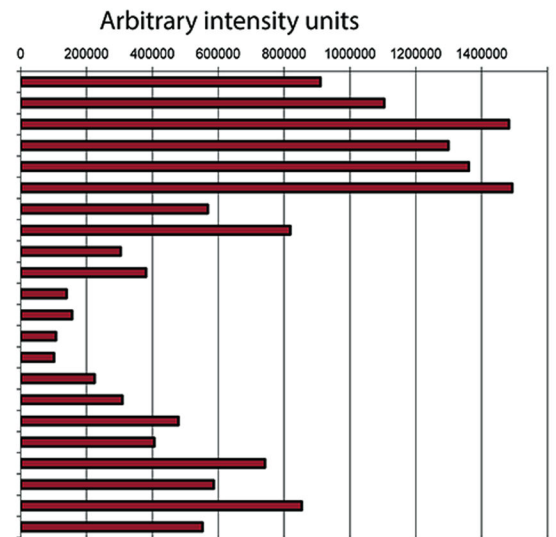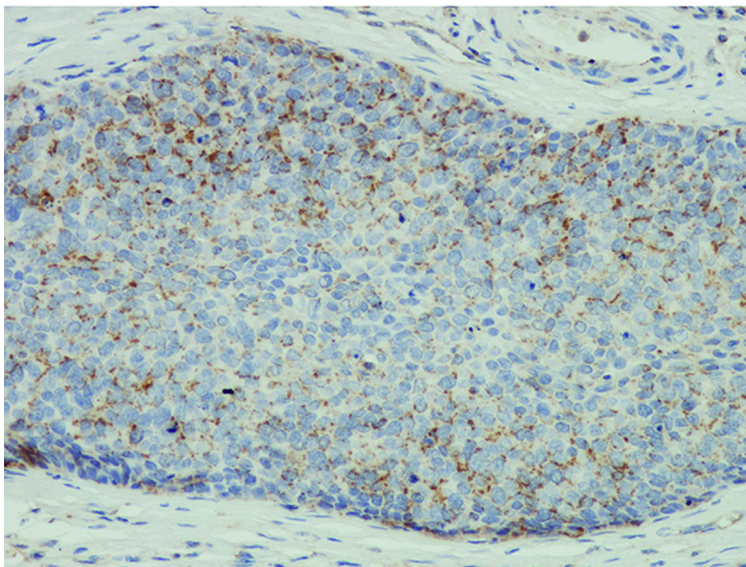
Figure 8.
Immunohistochemistry of serial sections of esophageal squamous cell carcinoma stained with CcO IVi1 (top) and Vb (bottom). Right panel shows densitometry of DAB staining pattern as described in Materials and methods available online in Supplemental information.